STUDIA UBB CHEMIA, LXX, 3, 2025 (p. 7-20)
(RECOMMENDED CITATION)
DOI:10.24193/subbchem.2025.3.01

ONLINE ELECTROCHEMICAL MONITORING OF PRODUCTS' CONCENTRATIONS DURING THE HBr AND KOH ELECTROSYNTHESIS BY ELECTRODIALYSIS

Gabriele-Mario BOGDAN[a], Sorin-Aurel DORNEANU[a,b,*]

ABSTRACT. In 2022, an estimated 62 billion kg of e-waste was generated, with an approximate value of $91 billion; however, the externalized and process costs of recycling make it economically unattractive. Our previous studies have demonstrated the possibility of electrochemically producing and regenerating the main reagents required for the Br_2/Br^- leaching system used in metals recovery from waste printed circuit boards. To facilitate the optimization of these processes, in this study, mathematical models were developed that enabled us to calculate concentration of KOH, H_2SO_4 and KBr from temperature and conductivity data and to determine the fitting parameters over the required concentration and temperature ranges using MATLAB's Curve Fitting Toolbox. The developed models were compared against pre-existing ones and literature data and were validated using experimental data gathered using a complex computer-controlled setup. For KOH and KBr, the adapted models provide an almost perfect fit between the obtained calibration surfaces and literature and experimental data. Contrarily, for H_2SO_4, a more complex 10-parameter model was developed to properly fit data in the desired range of temperature and concentration. Using the obtained fitting parameters, the possibility of online and in situ monitoring of target electrolyte concentrations using inexpensive conductivity and temperature sensors was confirmed.

Keywords: *mathematical model; conductivity; concentration monitoring; electrochemical sensors; WPCBs recycling process.*

[a] *Department of Chemical Engineering, Faculty of Chemistry and Chemical Engineering, Babeş-Bolyai University, 11 Arany Janos Street, RO-400028, Cluj-Napoca, Romania*
[b] *Interdisciplinary Research Institute on Bio Nano Sciences, Babeş-Bolyai University, 42 Treboniu Laurian Street, RO-400271, Cluj-Napoca, Romania*
[*] *Corresponding author: sorin.dorneanu@ubbcluj.ro*

INTRODUCTION

Technological progress and consumerism have turned e-waste into one of the largest pollution-related issues in modern times, with more than 62 billion kg generated in 2022. One of the most valuable components of e-waste are waste printed circuit boards (WPCBs) which — due to their high content of valuable metals — represent an extremely important resource for recycling, with an approximate value of $91 billion. Insufficiently ecological recycling processes, however, have led to an estimated externalized cost (the cost of bad societal outcomes related to pollution) of e-waste recycling of around $78 billion, with another $10 billion in operational costs [1]. Consequently, the development of more environmentally friendly and economically viable recycling processes is crucial for successful long-term and sustainable implementations of WPCB recycling technologies [2–5]. Though WPCB recycling technologies are very diverse [6], pyrometallurgical and mechanical recycling technologies can be very polluting, releasing heavy-metal containing particulate matter, greenhouse and toxic gases all of which can be very detrimental to human and environmental health [5,7]. As of 2024, approximately 46% of the global energy production capacity comes from renewable sources [8], meaning hydrometallurgical processes combined with electrochemical techniques present the highest potential in regards to sustainability and pollution reduction compared to pyrometallurgical or physical methods. Electrochemistry can be applied at almost every stage of the recycling process, starting from dissolving the metals using electrochemically regenerable leaching systems like $H_2SO_4/CuSO_4/NaCl$ [9] or Fe^{3+}/Fe^{2+} [10], followed by selective electroextraction of metals from solution [11,12] and electrochemical regeneration of reagents [13], allowing for a very sustainable, low-cost recycling system.

Our previous studies have demonstrated the feasibility of implementing the electrochemically regenerable Br_2/Br^- leaching system for complete metals recovery from WPCBs [14,15]. A flowchart of the proposed recycling process was developed during author Bogdan's Bachelor Thesis [16]. The main takeaway from the proposed flowchart is that, after the recycling process is concluded, the resulting secondary fluxes consist of two clean KBr solutions of concentration smaller than 2 M, one of which contains an unknown amount of HBr. Provided these KBr solutions are reconcentrated up to process requirements, which could be achieved through electrodialysis, they can be used as raw materials for the electrochemical reagent preparation and regeneration process. In this context, we previously demonstrated the possibility of profitably producing, by electrodialysis, KOH and HBr solutions at the required process concentrations using a 2 M KBr and a four-compartment filter press electrochemical reactor. During the electrosynthesis tests, solutions of 2 M KBr, 2 M H_2SO_4 and 0.1 M KOH were used in the reactor's compartments' flow

circuits, with final concentrations of HBr and KOH of 0.768 and 0.893 M respectively. Consequently, for the complete monitoring of reagent concentrations in this process, in order to optimize the operating parameters and increase its profitability, this research focuses exclusively on adapting, improving and testing the viability of the mathematical model around the operating concentrations of products and reagents. Additionally, our preliminary results proved the possibility of using low-cost conductivity sensors for the online and in-situ monitoring of KOH concentrations between 0.1 ÷ 1 M [13]. Building on these promising results, the aims of this study are (i) to develop mathematical relationships that will allow the computation of, using real-time sensor data, reagent concentrations in all four electrodialysis reactor compartments using simple and inexpensive electrochemical sensors and (ii) to acquire conductivity data for KBr, H_2SO_4 solutions between 1.25 ÷ 2.5 M, and KOH solutions between 0.5 ÷ 1 M, for temperatures between 23 ÷ 40°C in order to validate the proposed mathematical model. The temperature and concentration ranges were chosen based on prior electrosynthesis efficiency and performance data [13]. Exceeding 40°C indicates excessive energy loss as heat, thus, this value was chosen to be the upper limit for this study.

Developing robust mathematical models able to accurately compute concentration using sensor data would help eliminate the labor-intensive processes of samples extraction and manual determination of solute concentrations that is currently required, thus reducing process labor, materials and operational costs through advanced automation, resulting in further reductions of recycling process costs.

RESULTS AND DISCUSSION

Mathematical modelling of calibration surfaces

Even if many commercially available concentration sensors are based on electrical conductivity (EC) and temperature (T) data, the subject is not very well treated in literature. For example, Shahid et al. [17] proposed a mathematical relationship for determining concentration of NaCl, methylene blue (MB) and methyl violet 2b as a function of measured T and EC reproduced below:

$$C_{xx} = \frac{EC_{xx}}{a + b \cdot EC_{xx} + c \cdot EC_{xx}^2 + d \cdot EC \cdot T_{xx} + e \cdot T_{xx}} \quad (1)$$

where a ÷ e represent the fitting coefficients, xx represents the species for which the fitting was performed (xx=KOH, H_2SO_4, KBr), EC is the electrical conductivity (in mS/cm), T is the temperature (in K) and C is the electrolyte concentration (in mol/L).

This model was implemented inside MATLAB's Curve Fitting Toolbox, which allowed the input of a custom equation and to choose the Levenberg – Marquardt algorithm for estimating the fitting coefficients based on available (EC, T, C) literature data for KOH [18], H_2SO_4 [19] and KBr [20]. The fitted coefficients obtained, the corresponding R^2 value (computed by MATLAB) and the applicable temperature, concentration and conductivity ranges are presented in Table 1.

Conductivity values must be constrained in order to remain within the model's applicable range using a first order equation EC=f(T), which was determined through linear regression in Excel for the upper concentration limit of each substance. For a wider range of temperatures or concentrations, higher degree polynomials might need to be determined and implemented for each substance.

Table 1. Fitted coefficients a÷e of equation (1) obtained for KOH, H_2SO_4, KBr and applicable for specified concentration, temperature and conductivity ranges.

Subst.	**KOH**	**H_2SO_4**	**KBr**
a	-0.566	-0.589	-0.505
b	-0.861	-0.828	0.159
$c \cdot 10^3$	2.599	2.660	0.591
$d \cdot 10^2$	-17.24	-19.10	-4.77
$e \cdot 10^3$	2.711	3.460	2.111
R^2	0.9999	0.9983	0.9999
T range [K]	273 ÷ 323	300 ÷ 344	288 ÷ 328
C range [M]	0 ÷ 1	0 ÷ 3.05	0 ÷ 3.18
EC range [mS]	$0 \div (2.82 \cdot 10^{-3} \cdot T - 0.62)$	$0 \div (5.05 \cdot 10^{-3} \cdot T - 1.16)$	$0 \div (1.09 \cdot 10^{-3} \cdot T - 2.45)$

The R^2 values indicate that Shahid's model could be successfully implemented for calculating KBr and KOH concentrations within the specified ranges, however the marginally lower value for H_2SO_4, combined with the narrower temperature range warrants further investigation. A visual comparison between the obtained surface and the literature data reveals a very large discrepancy between the two for temperatures under 300 K, with residuals reaching up to 1.2 M at 273 K. Including data from 273 – 300 K reduces the R^2 value to 0.938. Unfortunately, despite extensive adjustments to the many fitting options available in MATLAB's Curve Fitting Toolbox, no further improvement of the fitting was observed. In conclusion, Shahid's mathematical model is not suitable for determining H_2SO_4 concentration under the given conditions.

Further inspection of the fit between the surface obtained through the mathematical model and the literature data reveals that Shahid's model is unable to properly compensate for the strong curvature present at lower temperatures,

which is absent in the case of KBr and KOH at the specified concentration range. Existing models for conductivity as a function of concentration contain exponential or logarithmic terms in the form of $a \cdot C^n \cdot e^{b \cdot C}$ or $a \cdot C \cdot \log C$ respectively, terms which introduce an inflection point at one or more local maximums for specific concentrations and temperatures [21,22]. In the case of KOH the inflection point occurs at high concentrations, greater than 5 M [18], and in the case of KBr, above 15°C, conductivity varies monotonously over the entire concentration range [21,23], meaning that the exponential/logarithmic term is not very significant. In contrast, the EC = f(C) dependency of H_2SO_4 exhibits an inflection point at concentrations much closer to our range of interest, starting at around 3.5 M at 0°C, gradually shifting towards higher concentrations at elevated temperatures. A visual representation of the EC=f(C) dependency for KOH and H_2SO_4 at 25 °C superimposed with the target concentration ranges of this study is presented in Figure 1.

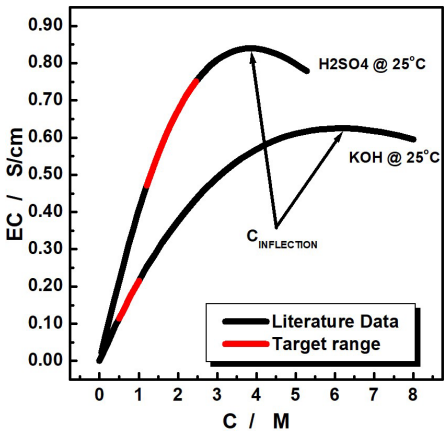

Figure 1. Dependency between conductivity and concentration for KOH and H_2SO_4 (black) superimposed with the target concentration ranges of this study (red).

This can be explained by two main factors, (i) the lower mobility of the HSO_4^- and SO_4^{2-} anions compared to OH^- or Br^- and (ii) the high dissociation factor of the second proton of H_2SO_4 at low concentrations and it's reassociation at higher concentrations respectively. It's widely accepted that, up to around 80 wt%, the first proton of sulfuric acid is completely dissociated, meaning that the dissociation factor of the second proton will play an important role towards changes in conductivity of sulfuric acid solutions. Spectroscopic investigations of sulfuric acid over a wide range of temperature and composition have shown that the dissociation factor of the second proton rises quickly between 10 ÷ 20% wt% H_2SO_4/H_2O, however its increase slows down and plateaus around 27 wt% H_2SO_4/H_2O at 290 K, decreasing at higher concentrations [24]. This behavior is consistent with the variation of conductivity

with concentration observed for H_2SO_4. Consequently, this behavior influences the allure of the EC = f(C) plot, resulting in a strongly exponential character of the C = f(EC) relationship around the studied concentration range.

Using these insights, an enhanced mathematical model that extends Shahid's model to be able to accurately determine concentrations for conductivity values close to the inflection point of the EC = f(C) relationship was proposed. This was done by first expanding the polynomial equation under the fraction to a complete linear combination of second order EC and T terms followed by the addition of the exponential $k \cdot T^n$ term which should be able to compensate for the strong curvature present near the inflection point, alongside other additional terms which were needed in order to obtain a better fit for portions where the exponential term's influence is not as large. Our proposed mathematical model is presented in equation (2):

$$C_{xx} = \frac{a \cdot EC_{xx} + b \cdot T_{xx}}{c + d \cdot EC_{xx} + e \cdot EC_{xx}^2 + f \cdot EC_{xx} \cdot T_{xx} + g \cdot T_{xx} + h \cdot T_{xx}^2 + k \cdot T_{xx}^n} \quad (2)$$

where EC, T, C and xx have the same meaning as described for equation (1). Using the same method described above, fitting coefficients were re-evaluated for all three substances and presented in Table 2.

Table 2. Fitted coefficients a÷n of equation (2) obtained for KOH, H_2SO_4, KBr.

Subst.	a	$b \cdot 10^5$	c	d	e	$f \cdot 10^3$	$g \cdot 10^2$	$h \cdot 10^5$	k	n	R^2
KOH	4.727	0.051	-0.411	-2.306	-0.267	5.794	-0.347	2.926	-	-	1.0000
H_2SO_4	1.927	8.619	0.360	-2.041	-0.185	5.419	16.87	-11.75	-0.853	0.672	0.9985
KBr	19.11	-6.298	-1.605	4.535	-1.442	-15.01	-1.376	8.984	-	-	1.0000

In the case of KOH and KBr, where the target concentrations are not close to an inflection point, the exponential term $k \cdot T^n$ is negligible and thus can be ignored in order to allow for simpler and faster calculation. An improvement in the R^2 value can be observed for all three substances, with a perfect fit ($R^2 = 1.0000$) for KOH and KBr. The applicable temperature range for H_2SO_4 increased from 300 ÷ 344 K to 278 ÷ 366 K, showing the great improvement of the model. Critically, because n takes a value below 1, the $k \cdot T^n$ term grows slower than the first and second order polynomial terms, meaning that its influence will diminish at higher temperatures. This is consistent with the real behavior of electrolyte solutions, where the inflection points of the EC = f(C) plot moves to higher concentrations at elevated temperatures, sometimes moving past the electrolyte's saturation limit. Though this study only validates

the model for H_2SO_4, we believe it could be successfully implemented for other electrolytes which exhibit an inflection point close to the target concentration range. Also, it is very important to note that, by inverting the EC = f(C) relationship, the resulting C = f(EC) function is bijective only up to the concentration $C_{inflection}$, where the derivative dEC/dC is equal to 0. If concentration needs to be calculated for the entire range up to the saturation point, fitting coefficients need to be determined for points pre/post $C_{inflection}$, and another property of the solution which varies monotonously with concentration up to the saturation point (such as density) must be used in order to determine which side of the inflection point you are on and, consequently, which of the equations to use.

Using the fitted coefficients and equation (2), calibration surfaces, presented in Figure 2, were generated for concentration and conductivity ranges mentioned in Table 1, covering a temperature range of 293 ÷ 323 K. These surfaces enable real-time concentration estimation from sensor data within the studied ranges.

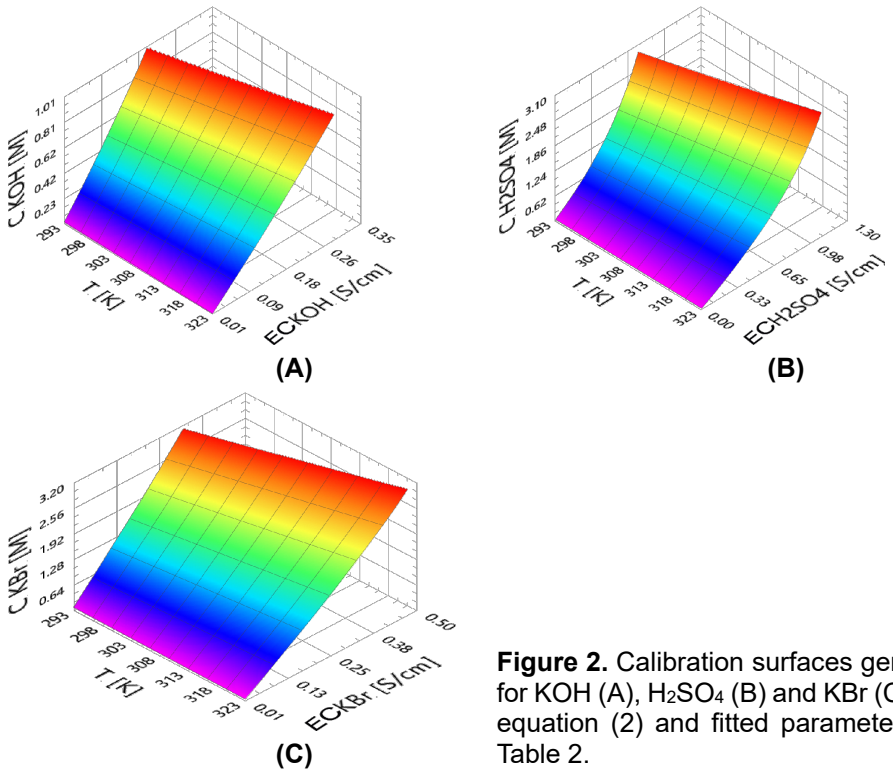

Figure 2. Calibration surfaces generated for KOH (A), H_2SO_4 (B) and KBr (C) using equation (2) and fitted parameters from Table 2.

Validation of calibration surfaces

In order to validate our mathematical model, conductivity measurements were performed for KOH, H_2SO_4 and KBr at 11 concentrations and 3 temperatures using a complex computer-controlled experimental setup (see Experimental Section), resulting in 3 sets of 33 (EC, T, C) points per substance to be used for comparison. Experimental temperature and conductivity data were input into our and Shahid's models and corresponding concentrations were computed. A comparison between (i) experimental data, (ii) Shahid's model and (iii) our model against reference literature data is presented in Figure 3.

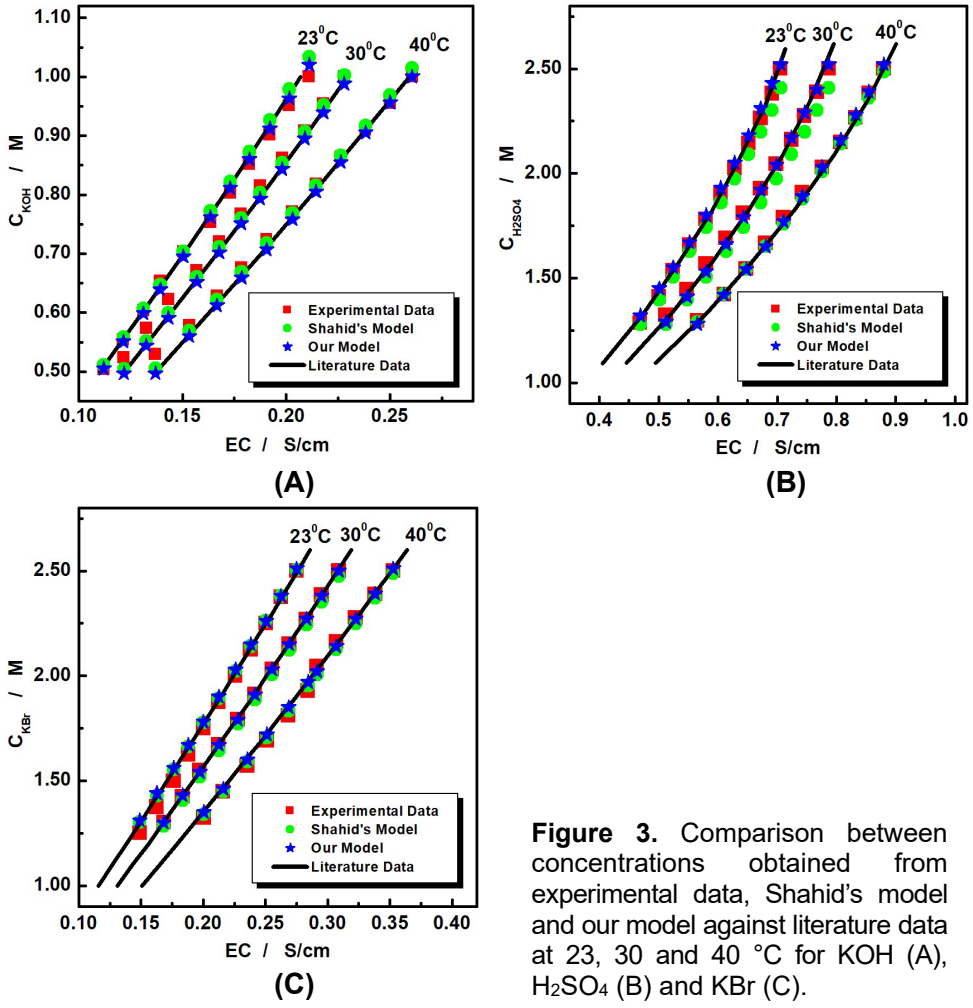

Figure 3. Comparison between concentrations obtained from experimental data, Shahid's model and our model against literature data at 23, 30 and 40 °C for KOH (A), H_2SO_4 (B) and KBr (C).

For a quantitative comparison of the model's performance and experimental accuracy, three statistical metrics, R^2, R (accuracy rate) and SSE (sum of squares error), were evaluated against reference literature data using the following equations:

$$R^2 = 1 - \frac{\sum_1^i \left(y_{i,d} - f_{i,lit} \right)^2}{\sum_1^i \left(y_{i,d} - \overline{y_{i,lit}} \right)^2} \tag{3}$$

$$R = \frac{1}{11} \cdot \sum_1^i \frac{1 - \left| y_{i,d} - f_{i,lit} \right|}{y_{i,d}} \tag{4}$$

$$SSE = \sum_1^i \left(y_{i,d} - f_{i,lit} \right)^2 \tag{5}$$

where i represents the index of the data point, $y_{i,d}$ represents the i-th concentration value of the considered dataset d (experimental, Shahid's model, our model), $f_{i,lit}$ represents the concentration calculated for the i-th measured conductivity through polynomial regression on literature data and $\overline{y_{i,lit}}$ is the mean of the literature concentration values used for comparison. The calculated R^2, R and SSE values are presented in Table 3.

Table 3. Values of relevant statistical metrics evaluated by comparing experimental and model data against literature data for KOH, H_2SO_4 and KBr at 23, 30 and 40°C.

Subst.	Temp.	Experimental data			Shahid's model			Our model		
		R	R^2	SSE·10^2	R	R^2	SSE·10^2	R	R^2	SSE·10^2
KOH	23°C	0.993	0.986	0.199	0.999	0.993	0.037	0.999	0.993	0.035
	30°C	0.985	0.975	0.371	0.998	0.991	0.053	1.000	0.996	0.011
	40°C	0.992	0.983	0.198	0.998	0.990	0.055	0.999	0.995	0.017
H_2SO_4	23°C	0.997	0.991	0.520	0.964	0.972	5.116	0.998	0.990	0.419
	30°C	0.992	0.983	1.219	0.951	0.968	6.943	0.999	0.994	0.240
	40°C	0.998	0.992	0.349	0.999	0.996	0.083	0.999	0.994	0.190
KBr	23°C	0.995	0.985	0.932	0.999	0.995	0.093	0.999	0.993	0.190
	30°C	1.000	0.997	0.043	0.994	0.986	0.884	1.000	0.998	0.032
	40°C	0.995	0.986	0.867	0.997	0.989	0.487	1.000	0.998	0.022

As anticipated, our model demonstrates only marginal improvements over Shahid's model for KOH and KBr, since the studied concentration intervals are far away from the inflection point. A substantial improvement in

the fit is observed for H_2SO_4, with R^2 values very close to 1, and SSE values more than 10 to 30 times lower at 23 and 30°C respectively. These results confirm that our additional terms effectively compensate for the pronounced curvature present near the inflection point.

CONCLUSIONS

This study successfully developed enhanced mathematical models for real-time concentration determination in solutions of KOH, H_2SO_4 and KBr used in the Br_2/Br^- metals recovery system from WPCBs through temperature and conductivity measurements. The equation parameters required to calculate concentrations based on temperature and conductivity data for KOH, H_2SO_4 and KBr were determined by building upon a model proposed by Shahid et al, improving it by expanding its viability for concentrations close to the inflection point of the EC = f(C) dependency. Literature and experimental data acquired through a complex experimental setup were used to successfully validate the fitted parameters we obtained for our models, thus proving the possibility of implementing electrochemical sensors for online monitoring and control of certain inorganic electrosynthesis processes. Further developments and improvements to these models should focus on testing the possibility of using them to monitor other electrolytes' concentrations and finding other solution properties which could be used to determine the measurement's position in regards to the inflection point, thus widening the applicable operating range of the models. These new models will gain significant relevance for potential industrial applications concerning the electrochemical monitoring of inorganic reagents concentrations obtained by electrosynthesis.

EXPERIMENTAL SETUP

Reagents

All chemicals were of analytical grade (purity >99%) unless otherwise specified. Solid KBr, KOH and methylene blue (MB) used in the preparation of stock 2.5 M KBr, 1 M KOH and 400 μM MB were purchased from Merck, Germany. The 2.5 M H_2SO_4 stock solution was prepared using 98% H_2SO_4 from Chempur, Germany. All solutions were prepared using double distilled water produced by a laboratory-grade water distillation system.

Equipment

The experimental setup used the following commercial equipment: one SP10T pH/T combined sensor (Consort, Belgium), one LM35 semiconductor-based temperature sensor, one SK23T conductivity sensor (Consort, Belgium), two Reglo Digital MS-2/8 peristaltic pumps called P.P.1 and P.P.2 (ISMATECH, Switzerland), one NI PCI-6259M data acquisition board (National Instruments, USA) inside of a pre-built computer, one USB4000 modular UV-VIS diode array spectrophotometer, two QP600-025-SR UV optical fibers, a FIA-Z-SMA-PEEK flow spectrophotometric cell with 10 mm optical path, a UV-VIS-NIR DT-MINI-2-GS light source all from Ocean Optics, USA, one Thermomix UB thermostat (B. Braun, Germany) and auxiliary equipment such as tubes, stirrers, etc.

Besides commercial equipment, proprietary equipment developed by author S.-A. Dorneanu was integrated in the experimental setup. Our custom equipment was able to interface with the sensors and the computer, allowing for the simultaneous acquisition of conductivity, pH, spectral and temperature data.

Experimental setup

A simplified schematic of the experimental setup employed is presented in Figure 4. The setup consists of a 75 mL double-walled mixing cell connected to a thermostatically controlled water bath and equipped with a lid which had holes for sensors and tubes. Conductivity, pH and T sensors were placed in the appropriate holes, alongside the connecting tubes of P.P.1 and P.P.2. The tubes were positioned inside of the cell such that it allowed for the bidirectional flow of liquid pumped by P.P.2, yet allowed only unidirectional flow from the tank of water dyed with methylene blue (T-W+MB) towards the mixing cell for P.P.1. The EC, pH and T sensors were connected to our proprietary equipment, which was then connected to the data acquisition board using a 68-pin cable. The pumps, magnetic stirrer, light source and spectrophotometer were controlled using a dedicated LabVIEW application. Thermoregulation required manual temperature adjustments between measurements because of the thermostat's limited interface capabilities.

To begin the experiment, 25 mL of stock solution of the target substance was transferred into the dry mixing cell using a calibrated pipette, after which it was given time to reach the target temperature under stirring. Meanwhile, pump P.P.2 was vehiculating the solution through the Z-cell, in order for the external fluid channels to reach thermal equilibrium with the solution inside the mixing cell. Once the desired temperature was reached, using the LabVIEW application, the black (baseline) and blank signals were acquired simultaneously with the conductivity and temperature values at the time when the spectroscopic measurement was taken. In order to improve measurement accuracy, each data

point represented the average of 10 measurements taken over the course of 3 seconds. After the first measurement, P.P.1 starts pumping a pre-determined volume of water dyed with methylene blue, which was calculated such that, after 10 additions, the concentration of the solution will be halved and the concentration values would be evenly distributed across the test range. After each dyed water addition, the software waited for the solution to reach the desired temperature and repeated the acquisition steps from the first measurement, except registering the black signal. The tube used for the peristaltic pump P.P.1 was calibrated before and after each experiment by running it at maximum speed for 1 minute and reading the volume pumped on the graduated pipette.

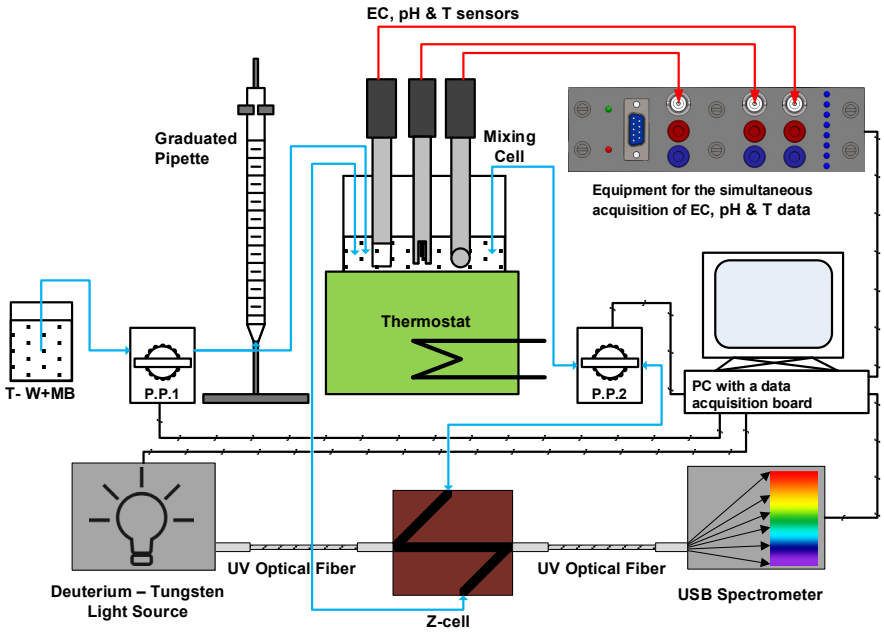

Figure 4. Simplified schematic of the experimental setup used for the acquisition of temperature, conductivity, pH and spectral data for KOH, H_2SO_4 and KBr.

Experimental concentrations after each addition were calculated based on pumping speed, pumping time and the tube calibration constant. In order to validate this approach, we implemented an innovative verification method utilizing methylene blue as a spectroscopic tracer. By measuring absorption at well-defined peaks, we calculated concentrations using the Lambert-Beer law and compared the concentrations obtained spectrophotometrically with

those obtained based on pumping parameters. Consequently, we prepared a 20 μM MB solution by diluting 50 mL of the 400 μM stock solution in 1 L of distilled water, which was then used for the dilution of the electrolyte solutions inside of the mixing cell, resulting in a range of MB concentrations between 0 ÷ 10 μM over the course of the experiments, range for which MB has a linear absorption characteristic.

Some of the key advantages of this method are that it can provide real-time validation of dilution accuracy, it enables the detection of potential systematic errors and it confirms the proper working of the entire experimental setup The concentrations calculated from the pumping parameters and the ones calculated using the Lambert-Beer law agree within 1%, proving that there were no major errors in the dilution setup.

ACKNOWLEDGEMENTS

Author Gabriele-Mario Bogdan is grateful to Babeș-Bolyai University for the Special Scholarship for Scientific Activity (2024-2025), contract number 35809/28.11.2024.

REFERENCES

1. C. P. Baldé; R. Kuehr; T. Yamamoto; R. McDonald; S. Althaf; G. Bel; O. Deubzer; E. Fernandez-Cubillo; V. Forti; V. Gray; S. Herat; S. Honda; G. Iattoni; D. S. Khetriwal; V. Luda di Cortemiglia; Y. Lobuntsova; I. Nnorom; N. Pralat; M. Wagner; *The Global E-waste Monitor 2024*, ITU & UNITAR, Geneva/Bonn, **2024**.
2. J. Lee; H. Choi; J. Kim; *Chem. Eng. J.*, **2024,** *494*, 152917.
3. A. M. Elgarahy; M. G. Eloffy; A. K. Priya; A. Hammad; M. Zahran; A. Maged; K. Z. Elwakeel; *Sustain. Chem. Environ.*, **2024**, *7*.
4. F. Cucchiella; I. D'Adamo; S. C. Lenny Koh; P. Rosa; *Renewable Sustainable Energy Rev.*, **2016**, *64*, 749–760.
5. R. Wang; Q. Zhang; L. Zhan; Z. Xu; *Environ. Pollut.*, **2022**, *308*, 119704.
6. H. Vermeșan; A.-E. Tiuc; M. Purcar; *Sustain.*, **2019**, *12*, 74.
7. S. Udayakumar; M. I. B. A. Razak; S. Ismail; *Mat. Today: Proc.*, **2022**, *66*, 3062–3070.
8. J. Prime; I. A. Ahmed; A. Dennis; N. Elhassan; Y. Melnikov; A. Whiteman; *Renewable capacity statistics 2025*, International Renewable Energy Agency, Abu Dhabi, **2025**.
9. C. Cocchiara; S.-A. Dorneanu; R. Inguanta; C. Sunseri; P. Ilea; *J. Cleaner Prod.*, **2019**, *230*, 170–179.
10. S. Fogarasi; F. Imre-Lucaci; A. Egedy; Á. Imre-Lucaci; P. Ilea; *Waste Manage.*, **2015**, *40*, 136–143.

11. M.-I. Frîncu; E. Covaci; S.-A. Dorneanu; P. Ilea; *Studia UBB Chemia*, **2020**, *65*, 33–44.
12. M. I. Frîncu; E. Covaci; S. A. Dorneanu; P. Ilea; *Studia UBB Chemia*, **2021**, *66*, 137–149.
13. G.-M. Bogdan; M. I. Frîncu; S.-A. Dorneanu; *Studia UBB Chemia*, **2024**, *69*, 177–191.
14. S. Varvara; S.-A. Dorneanu; A. Okos; L. M. Muresan; R. Bostan; M. Popa; D. Marconi; P. Ilea; *Mater.*, **2020**, *13*, 3630.
15. M.-I. Frîncu; G.-M. Bogdan; S.-A. Dorneanu; *Studia UBB Chemia*, **2025**, *70*, 7–22.
16. G.-M. Bogdan; *FCIC*, **2024**.
17. E. S. Shahid; S. H. Afzali; N. Talebbeydokhti; M. Rastegar; *Desalin. Water Treat.*, **2020**, *175*, 255–262.
18. R. J. Gilliam; J. W. Graydon; D. W. Kirk; S. J. Thorpe; *Int. J. Hydrogen Energy*, **2007**, *32*, 359–364.
19. H. E. Darling; *J. Chem. Eng. Data*, **1964**, *9*, 421–426.
20. T. Isono; *J. Chem. Eng. Data*, **1984**, *29*, 45–52.
21. B. B. Owen; H. Zeldes; *J. Chem. Phys.*, **1950**, *18*, 1083–1085.
22. S. Naseri Boroujeni; X. Liang; B. Maribo-Mogensen; G. M. Kontogeorgis; *Ind. Eng. Chem. Res.*, **2022**, *61*, 3168–3185.
23. H. E. Gunning; A. R. Gordon; *J. Chem. Phys.*, **1943**, *11*, 18–20.
24. C. E. Lund Myhre; D. H. Christensen; F. M. Nicolaisen; C. J. Nielsen; *J. Phys. Chem. A*, **2003**, *107*, 1979–1991.